

# Precise measurement of spin-averaged $\chi_{cJ}(1P)$ mass using photon conversions in $\psi(2S) \rightarrow \gamma\chi_{cJ}$

M. Ablikim<sup>1</sup>, J. Z. Bai<sup>1</sup>, Y. Ban<sup>11</sup>, J. G. Bian<sup>1</sup>, X. Cai<sup>1</sup>, J. F. Chang<sup>1</sup>, H. F. Chen<sup>17</sup>, H. S. Chen<sup>1</sup>, H. X. Chen<sup>1</sup>, J. C. Chen<sup>1</sup>, Jin Chen<sup>1</sup>, Jun Chen<sup>7</sup>, M. L. Chen<sup>1</sup>, Y. B. Chen<sup>1</sup>, S. P. Chi<sup>2</sup>, Y. P. Chu<sup>1</sup>, X. Z. Cui<sup>1</sup>, H. L. Dai<sup>1</sup>, Y. S. Dai<sup>19</sup>, Z. Y. Deng<sup>1</sup>, L. Y. Dong<sup>1a</sup>, Q. F. Dong<sup>15</sup>, S. X. Du<sup>1</sup>, Z. Z. Du<sup>1</sup>, J. Fang<sup>1</sup>, S. S. Fang<sup>2</sup>, C. D. Fu<sup>1</sup>, H. Y. Fu<sup>1</sup>, C. S. Gao<sup>1</sup>, Y. N. Gao<sup>15</sup>, M. Y. Gong<sup>1</sup>, W. X. Gong<sup>1</sup>, S. D. Gu<sup>1</sup>, Y. N. Guo<sup>1</sup>, Y. Q. Guo<sup>1</sup>, Z. J. Guo<sup>16</sup>, F. A. Harris<sup>16</sup>, K. L. He<sup>1</sup>, M. He<sup>12</sup>, X. He<sup>1</sup>, Y. K. Heng<sup>1</sup>, H. M. Hu<sup>1</sup>, T. Hu<sup>1</sup>, G. S. Huang<sup>1b</sup>, X. P. Huang<sup>1</sup>, X. T. Huang<sup>12</sup>, X. B. Ji<sup>1</sup>, C. H. Jiang<sup>1</sup>, X. S. Jiang<sup>1</sup>, D. P. Jin<sup>1</sup>, S. Jin<sup>1</sup>, Y. Jin<sup>1</sup>, Yi Jin<sup>1</sup>, Y. F. Lai<sup>1</sup>, F. Li<sup>1</sup>, G. Li<sup>2</sup>, H. H. Li<sup>1</sup>, J. Li<sup>1</sup>, J. C. Li<sup>1</sup>, Q. J. Li<sup>1</sup>, R. Y. Li<sup>1</sup>, S. M. Li<sup>1</sup>, W. D. Li<sup>1</sup>, W. G. Li<sup>1</sup>, X. L. Li<sup>8</sup>, X. Q. Li<sup>10</sup>, Y. L. Li<sup>4</sup>, Y. F. Liang<sup>14</sup>, H. B. Liao<sup>6</sup>, C. X. Liu<sup>1</sup>, F. Liu<sup>6</sup>, Fang Liu<sup>17</sup>, H. H. Liu<sup>1</sup>, H. M. Liu<sup>1</sup>, J. Liu<sup>11</sup>, J. B. Liu<sup>1</sup>, J. P. Liu<sup>18</sup>, R. G. Liu<sup>1</sup>, Z. A. Liu<sup>1</sup>, Z. X. Liu<sup>1</sup>, F. Lu<sup>1</sup>, G. R. Lu<sup>5</sup>, H. J. Lu<sup>17</sup>, J. G. Lu<sup>1</sup>, C. L. Luo<sup>9</sup>, L. X. Luo<sup>4</sup>, X. L. Luo<sup>1</sup>, F. C. Ma<sup>8</sup>, H. L. Ma<sup>1</sup>, J. M. Ma<sup>1</sup>, L. L. Ma<sup>1</sup>, Q. M. Ma<sup>1</sup>, X. B. Ma<sup>5</sup>, X. Y. Ma<sup>1</sup>, Z. P. Mao<sup>1</sup>, X. H. Mo<sup>1</sup>, J. Nie<sup>1</sup>, Z. D. Nie<sup>1</sup>, S. L. Olsen<sup>16</sup>, H. P. Peng<sup>17</sup>, N. D. Qi<sup>1</sup>, C. D. Qian<sup>13</sup>, H. Qin<sup>9</sup>, J. F. Qiu<sup>1</sup>, Z. Y. Ren<sup>1</sup>, G. Rong<sup>1</sup>, L. Y. Shan<sup>1</sup>, L. Shang<sup>1</sup>, D. L. Shen<sup>1</sup>, X. Y. Shen<sup>1</sup>, H. Y. Sheng<sup>1</sup>, F. Shi<sup>1</sup>, X. Shi<sup>11c</sup>, H. S. Sun<sup>1</sup>, J. F. Sun<sup>1</sup>, S. S. Sun<sup>1</sup>, Y. Z. Sun<sup>1</sup>, Z. J. Sun<sup>1</sup>, X. Tang<sup>1</sup>, N. Tao<sup>17</sup>, Y. R. Tian<sup>15</sup>, G. L. Tong<sup>1</sup>, G. S. Varner<sup>16</sup>, D. Y. Wang<sup>1</sup>, J. Z. Wang<sup>1</sup>, K. Wang<sup>17</sup>, L. Wang<sup>1</sup>, L. S. Wang<sup>1</sup>, M. Wang<sup>1</sup>, P. Wang<sup>1</sup>, P. L. Wang<sup>1</sup>, S. Z. Wang<sup>1</sup>, W. F. Wang<sup>1d</sup>, Y. F. Wang<sup>1</sup>, Z. Wang<sup>1</sup>, Z. Y. Wang<sup>1</sup>, Zhe Wang<sup>1</sup>, Zheng Wang<sup>2</sup>, C. L. Wei<sup>1</sup>, D. H. Wei<sup>1</sup>, N. Wu<sup>1</sup>, Y. M. Wu<sup>1</sup>, X. M. Xia<sup>1</sup>, X. X. Xie<sup>1</sup>, B. Xin<sup>8b</sup>, G. F. Xu<sup>1</sup>, H. Xu<sup>1</sup>, S. T. Xue<sup>1</sup>, M. L. Yan<sup>17</sup>, F. Yang<sup>10</sup>, H. X. Yang<sup>1</sup>, J. Yang<sup>17</sup>, Y. X. Yang<sup>3</sup>, M. Ye<sup>1</sup>, M. H. Ye<sup>2</sup>, Y. X. Ye<sup>17</sup>, L. H. Yi<sup>7</sup>, Z. Y. Yi<sup>1</sup>, C. S. Yu<sup>1</sup>, G. W. Yu<sup>1</sup>, C. Z. Yuan<sup>1</sup>, J. M. Yuan<sup>1</sup>, Y. Yuan<sup>1</sup>, S. L. Zang<sup>1</sup>, Y. Zeng<sup>7</sup>, Yu Zeng<sup>1</sup>, B. X. Zhang<sup>1</sup>, B. Y. Zhang<sup>1</sup>, C. C. Zhang<sup>1</sup>, D. H. Zhang<sup>1</sup>, H. Y. Zhang<sup>1</sup>, J. Zhang<sup>1</sup>, J. W. Zhang<sup>1</sup>, J. Y. Zhang<sup>1</sup>, Q. J. Zhang<sup>1</sup>, S. Q. Zhang<sup>1</sup>, X. M. Zhang<sup>1</sup>, X. Y. Zhang<sup>12</sup>, Y. Y. Zhang<sup>1</sup>, Yiyun Zhang<sup>14</sup>, Z. P. Zhang<sup>17</sup>, Z. Q. Zhang<sup>5</sup>, D. X. Zhao<sup>1</sup>, J. B. Zhao<sup>1</sup>, J. W. Zhao<sup>1</sup>, M. G. Zhao<sup>10</sup>, P. P. Zhao<sup>1</sup>, W. R. Zhao<sup>1</sup>, X. J. Zhao<sup>1</sup>, Y. B. Zhao<sup>1</sup>, Z. G. Zhao<sup>1e</sup>, H. Q. Zheng<sup>11</sup>, J. P. Zheng<sup>1</sup>, L. S. Zheng<sup>1</sup>, Z. P. Zheng<sup>1</sup>, X. C. Zhong<sup>1</sup>, B. Q. Zhou<sup>1</sup>, G. M. Zhou<sup>1</sup>, L. Zhou<sup>1</sup>, N. F. Zhou<sup>1</sup>, K. J. Zhu<sup>1</sup>, Q. M. Zhu<sup>1</sup>, Y. C. Zhu<sup>1</sup>, Y. S. Zhu<sup>1</sup>, Yingchun Zhu<sup>1f</sup>, Z. A. Zhu<sup>1</sup>, B. A. Zhuang<sup>1</sup>, X. A. Zhuang<sup>1</sup>, B. S. Zou<sup>1</sup>.

(BES Collaboration)

<sup>1</sup> Institute of High Energy Physics, Beijing 100049, People's Republic of China

<sup>2</sup> China Center for Advanced Science and Technology(CCAST), Beijing 100080, People's Republic of China

<sup>3</sup> Guangxi Normal University, Guilin 541004, People's Republic of China

<sup>4</sup> Guangxi University, Nanning 530004, People's Republic of China

<sup>5</sup> Henan Normal University, Xinxiang 453002, People's Republic of China

<sup>6</sup> Huazhong Normal University, Wuhan 430079, People's Republic of China

<sup>7</sup> Hunan University, Changsha 410082, People's Republic of China

<sup>8</sup> Liaoning University, Shenyang 110036, People's Republic of China

<sup>9</sup> Nanjing Normal University, Nanjing 210097, People's Republic of China

<sup>10</sup> Nankai University, Tianjin 300071, People's Republic of China

<sup>11</sup> Peking University, Beijing 100871, People's Republic of China

<sup>12</sup> Shandong University, Jinan 250100, People's Republic of China

<sup>13</sup> Shanghai Jiaotong University, Shanghai 200030, People's Republic of China

<sup>14</sup> Sichuan University, Chengdu 610064, People's Republic of China

<sup>15</sup> Tsinghua University, Beijing 100084, People's Republic of China

<sup>16</sup> University of Hawaii, Honolulu, HI 96822, USA

<sup>17</sup> University of Science and Technology of China, Hefei 230026, People's Republic of China

<sup>18</sup> Wuhan University, Wuhan 430072, People's Republic of China

<sup>19</sup> Zhejiang University, Hangzhou 310028, People's Republic of China

<sup>a</sup> Current address: Iowa State University, Ames, IA 50011-3160, USA

<sup>b</sup> Current address: Purdue University, West Lafayette, IN 47907, USA

<sup>c</sup> Current address: Cornell University, Ithaca, NY 14853, USA

<sup>d</sup> Current address: Laboratoire de l'Accélérateur Linéaire, F-91898 Orsay, France

<sup>e</sup> Current address: University of Michigan, Ann Arbor, MI 48109, USA

<sup>f</sup> Current address: DESY, D-22607, Hamburg, Germany

Using photon conversions to  $e^+e^-$  pairs, the energy spectrum of inclusive photons from  $\psi(2S)$  radiative decays is measured by BESII at the Beijing Electron-Positron Collider. The  $\chi_{cJ}(1P)$  states ( $J=0,1,2$ ) are clearly observed with energy resolution between 2.3 to 3.8 MeV, and their masses and the spin-averaged  $\chi_{cJ}$  mass are determined to be  $M_{\chi_{c0}} = 3414.21 \pm 0.39 \pm 0.27$ ,  $M_{\chi_{c1}} =$

$$3510.30 \pm 0.14 \pm 0.16, M_{\chi_{c2}} = 3555.70 \pm 0.59 \pm 0.39 \text{ and } M(^3P_{cog}) = 3524.85 \pm 0.32 \pm 0.30 \text{ MeV}/c^2.$$

PACS numbers: 13.25.Gv, 12.38.Qk, 14.40.Gx, 13.40Hg

Precise measurements of the spectrum and the decay properties of charmonia are essential to test Potential QCD models and QCD based approaches [1]. There is renewed interest since the discovery of the  $X(3872)$  [2] and the observations of the expected  $\eta_C(2S)$  and  $h_C(^1P_1)$  states [3], and there has been recent progress, both theoretically and experimentally [4]. There are more accurate determinations of the charmonium mass spectrum and radiative transition rates using both a relativistic quark model with relativistic corrections of order  $v^2/c^2$  [5] and a potential model with a semirelativistic approach [6]. The  $\psi(2S)$  mass and width have been redetermined with an updated radiative correction [7], and newly measured with better precision [8]. In addition to previous measurements of  $\chi_{cJ}$  states [9], two  $\chi_{c0}$  measurements by E835 [10] and new  $\chi_{cJ}$  ( $J=0,1,2$ ) measurements by CLEO [11] have been recently published. Improved precision on  $\chi_{cJ}$  masses is important for the determination of the singlet-triplet splitting,  $M(^1P_1) - M(^3P_{cog})$ , which is predicted by lattice QCD and nonrelativistic QCD [12]. Here  $M(^3P_{cog})$  is the spin-averaged  $^3P_J$  mass for the  $\chi_{cJ}$  states ( $J=0,1,2$ ).

In this paper, results on the  $\chi_{cJ}$  masses ( $J=0,1,2$ ) and widths ( $J=0,1$ ) from a measurement of the energy spectrum of inclusive photons in  $\psi(2S)$  radiative decays, using photon conversions to improve the energy resolution, are presented. The measurement uses  $14 \times 10^6$   $\psi(2S)$  events collected with the upgraded Beijing Spectrometer (BESII) at the BEPC Collider.

The BESII detector is described elsewhere [13]. A vertex chamber (VC) surrounding the beam pipe provides coordinate information. Charged particle momenta are determined with a resolution of  $\sigma_p/p = 1.78\% \sqrt{1+p^2}$  ( $p$  in GeV/c) in a cylindrical drift chamber (MDC). Particle identification is accomplished by measurements of ionization ( $dE/dx$ ) in the MDC and time-of-flight (TOF) in a barrel-like array of 48 scintillation counters. The  $dE/dx$  resolution is  $\sigma_{dE/dx} = 8\%$ ; the TOF resolution is  $\sigma_{TOF} = 200$  ps for hadrons. A barrel shower counter (BSC) measures energies of photons with a resolution of  $\sigma_E/E = 21\%/\sqrt{E}$  ( $E$  in GeV). A solenoidal coil supplies a 0.4 Tesla magnetic field over the tracking volume.

A Geant3 based Monte Carlo (MC) SIMBES [14], which simulates the detector response including interactions of secondary particles in the detector material, is used to determine the energy resolution and detection efficiency of photons reconstructed from their converted  $e^+e^-$  pairs, as well as to optimize selection criteria and estimate backgrounds. Under the assumption of a pure E1 transition for the  $\psi(2S) \rightarrow \gamma\chi_{cJ}$ , the polar angle ( $\theta$ ) distributions of the photons are given by  $1 + k \cos^2 \theta$  with

$k = 1, -\frac{1}{3}, \frac{1}{13}$  for  $J = 0, 1, 2$ , respectively [15].

Good energy resolution for low energy photons is essential for precise measurements of  $\chi_{cJ}$  masses and widths from fitting the photon spectrum of  $\psi(2S)$  radiative decays. Momentum resolution of about 1.6 to 4.1 MeV/c can be obtained for low momentum electrons from 60 to 250 MeV/c. Photons from  $\psi(2S) \rightarrow \gamma\chi_{cJ}$  decays have energies of about 261, 171, and 128 MeV for the  $\chi_{cJ}$  final states ( $J=0,1,2$ ), and the electrons produced in photon conversions occur in this low momentum region.

We choose two oppositely charged tracks with each track having a good helix fit and a polar angle with  $|\cos \theta| < 0.8$ . The intersection of the electron and positron trajectories in the xy-plane (the beam line is the  $z$  axis) is determined, and this point is taken as the photon conversion point (CP). The photon conversion length  $R_{xy}$  is defined as the distance from the beam line to the CP in the xy-plane. Fig. 1 shows the  $R_{xy}$  distribution for photon conversions to  $e^+e^-$  pairs in the BESII detector for hadronic events in the  $58 \times 10^6$   $J/\psi$  event sample. The two broad peaks in Fig. 1 correspond to the beampipe region, where the beampipe, the VC, and inner wall of the MDC are located. Combinatorial background from charged hadron tracks is also seen in the  $R_{xy} < 2$  cm region. Equivalent materials in the beampipe wall, VC, VC outer wall, and the MDC inner wall are 0.536, 0.657, 0.375, and 1.107 in units of  $0.01X_0$  [16], respectively, where  $X_0$  is a radiation length. The electron and positron directions are calculated at the photon conversion point, and their momenta are corrected to that point.

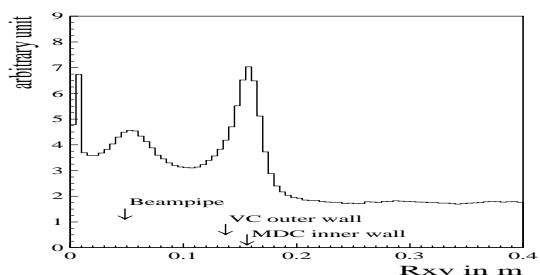


FIG. 1: The  $R_{xy}$  distribution for gamma conversions to  $e^+e^-$  pairs in the BESII detector from hadron events in the  $58 \times 10^6$   $J/\psi$  event sample.

Good photons are selected. The photon conversion length must lie within the beampipe region,  $2 < R_{xy} < 22$  cm, and the invariant mass of an  $e^+e^-$  pair is required to satisfy  $M_{e^+e^-} < 20 \text{ MeV}/c^2$ . Combinatorial background from charged hadron tracks is further removed by requiring  $\cos \theta_{defl} > 0.9$ , where  $\theta_{defl}$  is the deflection angle between the photon momentum and photon track

(a vector from the beam to the CP). To suppress background from beam-gas and beam-pipe interactions, the total energy in the event must satisfy  $E_{tot} > E_{beam}/2$  and momentum asymmetry must satisfy  $dp_{asym} < 0.9$ . Here  $dp_{asym}$  is defined as a ratio of the vector sum to the scalar sum of the momenta of all charged and neutral tracks in the event. The observed photon energy spectrum from the  $\psi(2S)$  data after the selection of good photons is shown in Fig. 2. The spectrum shows the  $\chi_{cJ}$  states plus a large background. The sharp drop at low energy is mainly caused by low photon detection efficiency.

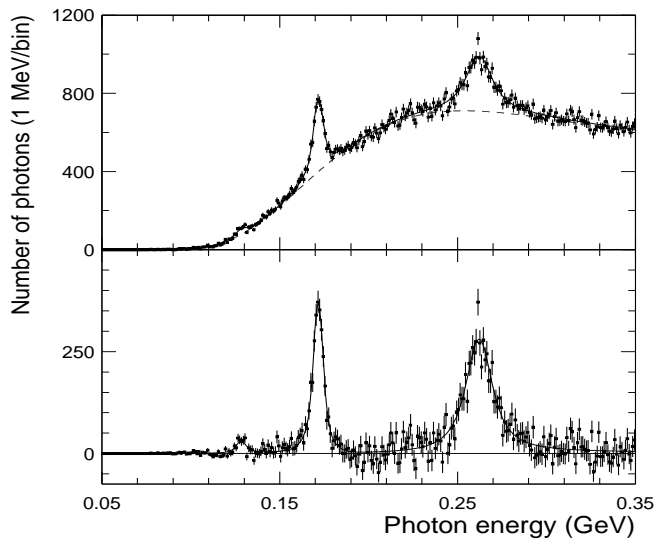


FIG. 2: Inclusive photon spectrum from photon conversions from  $14 \times 10^6$   $\psi(2S)$  events. A fit (described in the text) is made to  $\psi(2S) \rightarrow \gamma\chi_{cJ}$  decays ( $J = 0, 1, 2$ ) plus threshold background. Points with error bars are data. The solid line is the fit; the dashed line is the fitted background. Background subtracted results are shown in the lower plot.

Energy loss  $dE/dx$  by ionization for electrons traversing a small thickness of material with energy above a few tens of MeV can be described by the Bethe-Bloch equation [9]. The  $dE/dx$  correction for charged particles, produced near the beamline and traversing the whole beampipe region, should take into account the full thickness of material in the region. However,  $e^+e^-$  pairs from photon conversions are mostly produced in the region where the VC outer wall and the MDC inner wall are located. Thus the effective thickness of material between the location, where a pair is produced, and first layer of the MDC wires must be estimated for each electron pair. The procedure to make  $dE/dx$  corrections for electrons has two steps: (1) A preliminary  $dE/dx$  correction using half the full thickness of all the materials in the beampipe region is made. Good photons are reconstructed, and their conversion lengths  $R_{xy}$  are calculated. (2) The final  $dE/dx$  corrections are estimated based on these  $R_{xy}$ .

The energy scale of photons reconstructed from  $e^+e^-$  pairs is studied using simulated MC events and data.

A sample of  $\pi^0$  mesons decaying to two photons with both photons converting to  $e^+e^-$  pairs is selected from  $58 \times 10^6$   $J/\psi$  events. To suppress hadron contamination, electron identification is required and good photons are selected. Background is further suppressed with additional requirements on the photon energy,  $E_\gamma \leq 1\text{GeV}$ , and the opening angle between the two photons,  $0.75 < |\cos\theta_{\gamma\gamma}| < 0.97$ . The invariant mass distribution, after the specific  $dE/dx$  correction for electrons described above, is fitted with the improved Crystal Ball (ICB) function [17] plus a first order polynomial background. The resulting  $\pi^0$  mass ( $134.47 \pm 0.42$ ) MeV/ $c^2$  is consistent with the PDG value of 134.98 MeV/ $c^2$  [9].

The energy of a photon from  $\psi(2S) \rightarrow \gamma\chi_{cJ}$  decay is given by

$$E_\gamma = (M_{\psi(2S)}^2 - M_{\chi_{cJ}}^2)/2M_{\psi(2S)}, \quad (1)$$

where  $M_{\psi(2S)}$  and  $M_{\chi_{cJ}}$  are the masses of the  $\psi(2S)$  and  $\chi_{cJ}$ , respectively. The  $\psi(2S)$  and  $\chi_{cJ}$  widths must be taken into account;  $M_{\psi(2S)}$  and  $M_{\chi_{cJ}}$  are described by Breit-Wigner functions (2D problem). By taking  $x = M_{\psi(2S)}$ , the probability density function (pdf) for the photon energy  $E_\gamma$  can be written as [18]

$$f_{pdf}(E_\gamma) = \int BW(x)BW(M_{\chi_{cJ}})\frac{x}{M_{\chi_{cJ}}}dx, \quad (2)$$

where  $M_{\chi_{cJ}}$  depends on  $E_\gamma$  by Eq. (1).

As a result of traversing material in the beam pipe region, the electron energy is smeared due to energy loss by ionization, and a long tail on the low side of the energy distribution is induced by bremsstrahlung radiation. Multiple scattering of electrons, especially at large angles, gives tails on both sides of the photon energy distribution of photon conversions. The photon energy resolution from photon conversions can be nicely modeled by our Geant3 MC simulation, and well fitted by the ICB function. The photon energy distributions from large MC samples of  $\psi(2S) \rightarrow \gamma\chi_{cJ}$  decays ( $J = 0, 1, 2$ ), with zero widths for both the  $\psi(2S)$  and  $\chi_{cJ}$  states, are fitted to ICB functions. Five parameters in the ICB function, the photon energy resolution and four empirical parameters [17] to describe the tails on the lower and upper sides are determined from the fits and used as input parameters in the detector resolution function for each decay mode. Photon energy resolutions for the  $\psi(2S) \rightarrow \gamma\chi_{cJ}$  decays ( $J=0,1,2$ ) are found to be  $3.78 \pm 0.04$ ,  $2.58 \pm 0.05$ , and  $2.26 \pm 0.11$  MeV, respectively.

The energy dependencies of the photon detection efficiency and resolution are determined using MC simulation in the energy range between 100 and 400 (300, 220) MeV for  $\psi(2S) \rightarrow \gamma\chi_{c0}$  ( $\gamma\chi_{c1}, \gamma\chi_{c2}$ ) decays. The efficiency includes the effects of detector geometry, MDC tracking, photon reconstruction, and the spin-dependent  $\cos\theta$  distribution.

The smooth background under the signal photon lines can be described by a threshold function [17]. Contamination from  $\chi_{c0} \rightarrow \gamma J/\psi$  decay is negligible due to its small branching fraction. To exclude photons from the  $\chi_{c1,c2} \rightarrow \gamma J/\psi$  decays, the photon energy range in the fits is chosen to be within  $90 \text{ MeV} \leq E_\gamma \leq 350 \text{ MeV}$ . An enhancement from the decay  $\psi(2S) \rightarrow \eta J/\psi$  with  $\eta \rightarrow \gamma\gamma$  in a region of 180 to 400 MeV is estimated by MC method, and subtracted from the data, according to the measured total number of  $\psi(2S)$  events and known branching fractions.

An input-output test is performed to verify the accuracy of the fitting algorithm for the 2D problem using MC events. The energy dependencies of the photon detection efficiency and resolution are included in the fitting procedure. A sample of MC events for the  $\psi(2S) \rightarrow \gamma\chi_{cJ}$  decays with non-zero width for both the  $\psi(2S)$  and  $\chi_{cJ}$  are produced. The photon energy distribution is fitted with the 2D pdf function convoluted with the ICB resolution. The resulting masses and widths of the  $\chi_{cJ}$  states in this test are consistent with the MC input parameters.

A combined fit of the three photon spectra corresponding to the  $\psi(2S) \rightarrow \gamma\chi_{c0}, \gamma\chi_{c1}, \gamma\chi_{c2}$  decays is performed to three 2D pdf functions (see Eq. (2)), each convoluted with its ICB resolution function, plus threshold background. The  $\chi_{c2}$  width is fixed in the fit due to the limited statistics. The detection efficiency and energy resolution as a function of photon energy are included in the fitting. With the assumption that the  $E1$  electric dipole transition for  $\psi(2S) \rightarrow \gamma\chi_{cJ}$  decays ( $J=0,1,2$ ) dominates, an  $E_\gamma^3$  energy dependence is included in the folded signal shape. The effect of the beam energy spread [19] in the measurement is also included, but is found to be negligible due to the narrow width of the  $\psi(2S)$  state. A study shows that the bin size (0.5 or 0.2 MeV) in the binned fits slightly affects the fitted masses and widths of the  $\chi_{cJ}$  states. The difference in the results due to different bin sizes are added to the systematic error. The results of the binned fit (0.5 MeV/bin) are shown in Fig. 2.

Samples of QED radiative two photon events with one photon converting to an  $e^+e^-$  pair are selected for both data and MC simulation. The two photons are required to be emitted back-to-back. The fitted photon energy in data is different from the expected MC value by  $-1.2\sigma$  ( $\sigma = 0.86 \text{ MeV}$ ), which has a relative error at the same level as a correction factor  $s = 0.9975 \pm 0.0007$  for the magnetic field [20]. Thus a relative precision of 0.0007 is added as the systematic error in the photon energy determination.

The selection of  $\pi^0 \rightarrow \gamma\gamma$  events with both photons converting to  $e^+e^-$  pairs from  $58 \times 10^6 J/\psi$  events yields a data sample of 503  $\pi^0$  mesons. A MC sample of  $\pi^0$  mesons is generated with the same momentum and polar angular distributions as found from the  $\pi^0$  data sample. The  $\pi^0$  mass resolutions determined from the data and MC are in good agreement; their

difference is  $0.15 \pm 0.62 \text{ MeV}/c^2$ . We assume that the photon energy resolution and uncertainty in the direction of the photon momentum each contribute half in the  $\pi^0$  mass resolution. Hence, the difference  $\Delta\sigma_{M_{\pi^0}}$  of the  $\pi^0$  mass resolutions between MC and data from the uncertainty of the photon energy resolution lies within  $(-0.29, +0.59) \text{ MeV}/c^2$  with a probability of 68.3%. We assume  $\Delta\sigma_{E_\gamma}(\chi_{cJ})/\sigma_{E_\gamma}(\chi_{cJ}, MC) = \Delta\sigma_{M_{\pi^0}}/\sigma_{M_{\pi^0}}(MC)$ , where  $\sigma_{E_\gamma}(\chi_{cJ}, MC)$  and  $\Delta\sigma_{E_\gamma}(\chi_{cJ})$  are the MC photon energy resolution and the difference between MC and data for  $\chi_{cJ}$  final states, and  $\sigma_{M_{\pi^0}}(MC)$  and  $\Delta\sigma_{M_{\pi^0}}$  are  $\pi^0$  mass resolution in MC and the difference between MC and data. Thus  $1\sigma$  confidence intervals of  $\Delta\sigma_{E_\gamma}(\chi_{cJ})$  for the  $\psi(2S) \rightarrow \gamma\chi_{c0}, \gamma\chi_{c1}$  decays are estimated to be  $(-0.20, +0.40)$  and  $(-0.14, +0.27) \text{ MeV}$ , which are used to estimate systematic errors in the determination of the  $\chi_{c0}$  and  $\chi_{c1}$  widths.

The effect of the background shape uncertainty is studied using  $\psi(2S)$  data and  $\psi(2S) \rightarrow \text{anything}$  MC [21]. The relative differences in background shape parameters between floated and fixed widths of the  $\chi_{c0,c1}$  states are determined in fits for MC data, and fed back to correct background parameters in the fits for data. The difference between results for  $\psi(2S)$  data with the background shape floated and fixed is taken as a systematic error. In addition, our MC study with non-zero width of both  $\psi(2S)$  and  $\chi_{cJ}$  shows that differences in the fitted masses from input values for the  $\chi_{c0}$  and  $\chi_{c1}$  are  $0.12 \pm 0.06$  and  $0.06 \pm 0.03 \text{ MeV}/c^2$ , while that for the  $\chi_{c2}$  is as large as  $0.31 \pm 0.06 \text{ MeV}/c^2$ . The differences are attributed to uncertainties in the energy loss correction for low momentum electrons. The systematic errors, including the contributions from the uncertainties of the photon detection efficiency, are summarized in the Table I.

TABLE I: Summary of systematic errors in the determination of the  $\chi_{cJ}$  masses and widths (in  $\text{MeV}/c^2$ ).

source	$M_{\chi_{c0}}$	$\Gamma_{\chi_{c0}}$	$M_{\chi_{c1}}$	$\Gamma_{\chi_{c1}}$	$M_{\chi_{c2}}$
background shape	0.03	0.8	0.02	0.07	0.04
correction in magnetic field	0.19		0.13		0.09
MC simulation in $\sigma_{E_\gamma}$		$+0.29$ $-0.76$		$+0.25$ $-0.77$	
different bin size	0.02	0.02	0.01	0.01	0.02
photon energy correction	0.18		0.09		0.37
efficiency uncertainty	0.04	0.03	0.01	0.00	0.04
error of $M_{\psi(2S)}$	0.034		0.034		0.034
total	0.27	$+0.85$ $-1.10$	0.16	$+0.26$ $-0.77$	0.39

With good energy resolution for low energy photons obtained using photon conversions, the precise measurement of the masses and widths of  $\chi_{cJ}$  ( $J = 0, 1, 2$ ) states from inclusive  $\psi(2S)$  radiative decays can be obtained. The masses and widths are determined to be  $M_{\chi_{c0}} = 3414.21 \pm 0.39 \pm 0.27$ ,  $M_{\chi_{c1}} = 3510.30 \pm 0.14 \pm 0.16$ ,  $M_{\chi_{c2}} = 3555.70 \pm 0.59 \pm 0.39 \text{ MeV}/c^2$ ,  $\Gamma_{\chi_{c0}} =$

$12.6^{+1.5+0.9}_{-1.6-1.1}$  and  $\Gamma_{\chi_{c1}} = 1.39^{+0.40+0.26}_{-0.38-0.77}$  MeV/ $c^2$ . The mass splittings in the  $\chi_{cJ}(1P)$  triplet and their ratio are found to be  $\Delta M_{21} = M_{\chi_{c2}} - M_{\chi_{c1}} = 45.40 \pm 0.61 \pm 0.42$  MeV/ $c^2$ ,  $\Delta M_{10} = M_{\chi_{c1}} - M_{\chi_{c0}} = 96.09 \pm 0.41 \pm 0.31$  MeV/ $c^2$  and  $\rho(\chi_c) = \Delta M_{21}/\Delta M_{10} = 0.472 \pm 0.006 \pm 0.004$ . For the first time, the spin-averaged  $^3P_J$  mass (weighted with the factors  $2J+1$ ) for the  $\chi_{cJ}$  states is precisely measured in one experiment and determined to be  $M(^3P_{cog}) = 3524.85 \pm 0.32 \pm 0.30$  MeV/ $c^2$ . The first errors in the results are statistical and the second are systematic. Correlations are taken into account in the estimation of the  $M(^3P_{cog})$  systematic error.

The  $\chi_{cJ}$  masses ( $J=0,1,2$ ) determined here are consistent with the recent measurements by CLEO [11], but have smaller systematic errors. The precisions for the  $\chi_{c0}$  and  $\chi_{c1}$  masses are compatible with those of previous measurements by E835 [10] and E760 [9], while that for the  $\chi_{c2}$  mass is not as good as theirs due to low statistics. Note that our  $\chi_{c0}$  mass is lower than that measured by the E835 via  $\chi_{c0} \rightarrow \gamma J/\psi$  decay by 1.2 MeV (corresponding to  $1.8\sigma$ ), but agrees with their later measurement via  $\chi_{c0} \rightarrow \pi^0 \pi^0$  decay. The width of the  $\chi_{cJ}$  states ( $J=0,1$ ) determined here are also consistent with their values; larger errors in our widths are caused by limited statistics for both signal photons and inclusive  $\pi^0$  mesons.

The BES collaboration thanks the staff of BEPC for their hard efforts and the members of IHEP computing center for their helpful assistance, and also T.P. Li for helpful discussion on 2D pdf function. This work is supported in part by the National Natural Science Foundation of China under contracts Nos. 19991480, 10225524, 10225525, the Chinese Academy of Sciences under contract No. KJ 95T-03, the 100 Talents Program of CAS under Contract Nos. U-11, U-24, U-25, and the Knowledge Innovation Project of CAS under Contract Nos. U-602, U-34(IHEP); by the National Natural Science Foundation of China under Contract No. 10175060(USTC), and No. 10225522(Tsinghua University); and by the U.S. Department of Energy under Contract No. DE-FG02-04ER41291 (U Hawaii).

---

[1] E. Eichten *et al.*, Phys. Rev. D **21**, 203 (1980) and D **17**, 3090 (1978); V. A. Novikov, *et al.*, Phys. Rep. **41**, 1

(1978); C. Quigg and J. L. Rosner, Phys. Rep. **56**, 167 (1979); G. Bali, K. Schilling and A. Wachter, Phys. Rev. D **56**, 2566 (1997).

[2] Belle, S. K. Choi *et al.*, Phys. Rev. Lett. **91**, 262001 (2004). Babar, B. Aubert *et al.*, hep-ex/0406022.

[3] Belle, S. K. Choi *et al.*, Phys. Rev. Lett. **89**, 102001 (2002); CLEO, A. Tomaradze, hep-ex/0410090; E835, C. Patrignani, hep-ex/0410085.

[4] N. Brambilla *et al.*, Heavy Quarkonium Physics, hep-ph/0412158.

[5] D. Ebert, R. N. Faustov and V. O. Galkin, Phys. Rev. D **67**, 014027 (2003) and D **62**, 034014 (2000).

[6] S. F. Radford and W. W. Repko, hep-ph/0409290, Sep 24, 2004.

[7] OLYA and MD-1, A. S. Artamonov *et al.*, Phys. Lett. B **474**, 427 (2000).

[8] KEDR, V. M. Aulchenko *et al.*, Phys. Lett. B **573**, 63 (2003); BES, J. Z. Bai *et al.*, Phys. Lett. B **550**, 24 (2002);

[9] S. Eidelman *et al.* (Particle Data Group), Phys. Lett. B **592**, 1 (2004).

[10] E835, S. Bagnasco *et al.*, Phys. Lett. B **533**, 237 (2002); M. Andreotti *et al.*, Phys. Rev. Lett. **91**, 091801 (2003).

[11] CLEO, S. B. Athar *et al.*, Phys. Rev. D **60** 112002(2004). From their measured photon energies, one may estimate the  $\chi_{cJ}$  masses using Eq. (1) in the text.

[12] S. Godfrey and J. L. Rosner, Phys. Rev. D **66**, 014012(2002); S. Godfrey, hep-ph/0501083.

[13] BES, J. Z. Bai. *et al.*, Nucl. Instr. Meth. **A458**, 627 (2001); Nucl. Instr. Meth. **A344**, 319 (1994).

[14] H.M. Liu *et al.*, "The BESII Detector Simulation", to be submitted to NIM.

[15] G. Karl, S. Meshkov, and J.L. Rosner, Phys. Rev. D **13**, 1203 (1976).

[16] T. Hong *et al.*, High Energy Phys. and Nucl. Phys., V **25**, 617 (2001).

[17] The original Crystal Ball (CB) function has a Gaussian in its central and upper energy region but long tail at lower energy region. The improved CB function is defined as same as the CB function but has an additional tail at its upper side. See also I.C. Brock, A Fitting and Plotting Package Using MINUIT, version 4.07, Dec. 22th, 2000.

[18] M. Fisz, Probability and Mathematic Statistics, Berlin, 1958.

[19] The spread in the center-of mass energy at  $\psi(2S)$  energy is 1.3 MeV. See also BES Collab., Phys. Lett. B **550**, 24 (2002).

[20] A correction factor  $s = 0.9975 \pm 0.0007$  for magnetic field at the BESII is determined with mass measurement of the  $J/\psi$  reconstructed from  $\psi(2S) \rightarrow \pi^+ \pi^- J/\psi$  and  $J/\psi \rightarrow \mu^+ \mu^-$  decays.

[21] J.C. Chen *et al.*, Phys. Rev. D **62**, 034003 (2000).